Nanogenerators: An emerging technology towards nanoenergy

Yunlong Zi and Zhong Lin Wang

Citation: APL Materials **5**, 074103 (2017); doi: 10.1063/1.4977208
View online: http://dx.doi.org/10.1063/1.4977208
View Table of Contents: http://aip.scitation.org/toc/apm/5/7
Published by the American Institute of Physics

APL MATERIALS **5**, 074103 (2017)

Nanogenerators: An emerging technology towards nanoenergy

Yunlong Zi[1] and Zhong Lin Wang[1,2,a]
[1]*School of Materials Science and Engineering, Georgia Institute of Technology, Atlanta, Georgia 30332, USA*
[2]*Beijing Institute of Nanoenergy and Nanosystems, Chinese Academy of Sciences, National Center for Nanoscience and Technology (NCNST), Beijing 100083, People's Republic of China*

(Received 13 January 2017; accepted 10 February 2017; published online 1 March 2017)

Nanoenergy is a field of studying the small-scale, highly efficient energy harvesting, storage, and applications by using nanomaterials and nanodevices. Nanogenerators are developed to harvest these small-scale energies in the ambient environment, which were first invented in our group in 2006. In the past decade, we have developed nanogenerators based on piezoelectric and triboelectric effects for mechanical energy harvesting, and those based on pyroelectric and thermoelectric effects for thermal energy harvesting. We also explored other novel nanogenerators such as that based on ion streams. The proposed nanogenerators will facilitate the development of self-powered systems, which enables efficient energy utilization and sustainable operations of mobile devices for "smart" wearable technology, health monitoring, biomedical sensing, environmental protection, and even security.
[http://dx.doi.org/10.1063/1.4977208]

In the past two decades, with the rapid growth of the Internet of Thing (IoT), enormous small electronics such as sensors, actuators, and wireless transmitters have been integrated into every corner of this world for health monitoring, biochemical detection, environmental protection, remote controls, wireless transmission, and security. Each of these devices requires only small scale power in microwatt (μW) to milliwatt (mW) level, which also demands the power source with the characteristics of mobility, sustainability, and availability. Traditionally, batteries are commonly used to power these devices. However, monitoring, managing, and recycling the large quantities of batteries with limited lifetime are extremely difficult tasks, and the waste hazard chemicals left in the exhausted batteries has become another crucial threaten to the environment. The field of nanoenergy, as first proposed by our group, is targeting to provide sustainable small-scale power solutions for these devices.[1,2] This concept of nanoenergy is quite different from the large grid-scale power in megawatt (MW) or gigawatt (GW) as required for a country, a city, or an airplane (Figure 1(a)).

Conventional approaches for power generations are conducted by electromagnetic generators (EMGs) based on Faraday's law of electromagnetic induction, which was invented in 1831. However, this power generation technology can only effectively harvest high-frequency mechanical energies.[3] A broader range of energy source in the ambient environment, such as low-frequency mechanical energies including water waves, human body motions, and various energies in other forms such as thermal energy and chemical energy, cannot be effectively harvested through EMGs. To effectively convert these different small-scale energies into electrical output, we have invented the first nanogenerator (NG) in 2006[4] and developed various types of NGs in the past decade, based on the effects of piezoelectric,[4] triboelectric,[5] pyroelectric,[6] thermoelectric,[7] ion streams,[8] etc. Furthermore, a self-powered system can be integrated by NGs with energy storage units such as batteries and supercapacitors, for powering functional devices.[9] Thus in this system the energy harvested by the NGs can

[a]Author to whom correspondence should be addressed. Electronic mail: zhong.wang@mse.gatech.edu

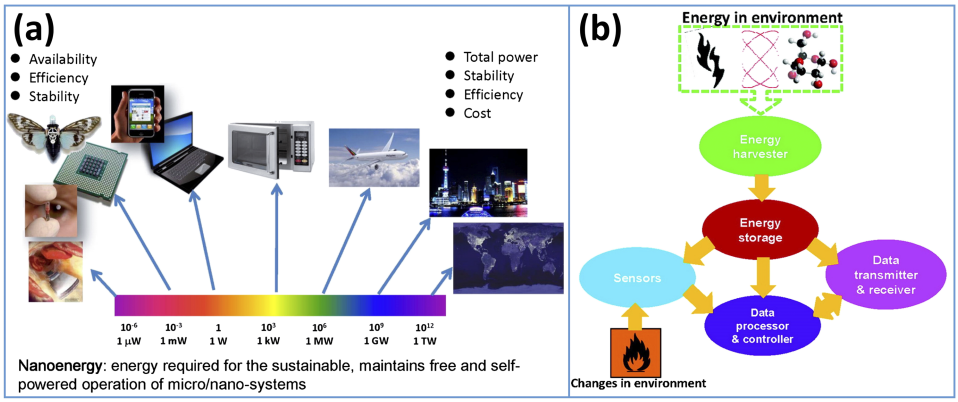

FIG. 1. (a) The power levels and corresponding applications. (b) The energy conversion process including energy harvesting by nanogenerators, energy storage, and applications. Reproduced with permission from Z. L. Wang, ACS Nano **7**(11), 9533 (2013). Copyright 2013 The American Chemical Society and Hu *et al.*, Nano Lett. **11**(6), 2572 (2011). Copyright 2011 The American Chemical Society.[2,9]

be temporarily stored in energy storage units, and then the energy will be available for applications including environmental sensing, data transmission, data processing, and controlling (Figure 1(b)).

In this report, we reviewed the development of various NGs in the past decade. Piezoelectric NG (PENG)[4] and triboelectric NG (TENG)[5] are two main members in the NG family for harvesting mechanical energy which is ubiquitously abundant in the ambient environment. Utilizing the strain-induced piezoelectric polarization in materials, PENG became the very first type of NGs we invented, and it has been developed with novel integrations,[10–13] advanced materials,[14–17] and varieties of demonstrated applications. As an emerging NG technology by coupling triboelectrification and electrostatic induction effects, TENG has been rapidly developed to be a promising mechanical energy harvester with four modes of operations,[18–20] and it has shown capability to harvest all the types of mechanical energies from water waves,[21–24] human motions,[25–27] vibrations,[28,29] wind,[30,31] etc. TENG has also demonstrated special advantages in efficiency for harvesting low-frequency mechanical energy.[3] Pyroelectric NG (PyENG)[6] and thermoelectric NG (ThENG)[7] are two types of NGs for thermal energy harvesting based on distinct mechanisms, which show their own characteristics in different application areas. Other types of NGs such as that based on ion stream effect are also being developed.[8] The development of these NGs provides the possibility of sustainable, maintenance-free, and self-powered operations of devices in the IoT, towards "smart" devices and systems in future.

Various types of materials, such as wurtzite materials, zinc blende materials, perovskite materials, and even polymers, have shown the piezoelectric effect. These materials have one important feature in common: dipole moments created by naturally formed positive and negative charge centers. As an example, we use wurtzite ZnO model (Figure 2(a)) to illustrate the origin of the piezoelectricity in the binary semiconductor materials. The crystal unit cell consists of one Zn^{2+} cation and one O^{2-} anion is illustrated as the dashed tetrahedral shape in Figure 1(a)-I. Under no strain condition, the Zn^{2+} cations (in the center of the unit cell) with the positive charge are overlapped with the center of the O^{2-} anions (in the corners of the unit cell) with negative charges (Figure 2(a)-II). If a strain exists along the *c*-axis, the centers of the cations and anions are displaced, which misaligns the positive and negative charges (Figure 2(a)-III). This misalignment leads to the varied dipole moment. The addition of the dipole moment in each crystal unit cell results in the additional polarization density, which is the reason for the piezopotential.[32] The ratio between the piezopotential and the strain applied is called the piezoelectric coefficient. Previously, our group has calculated the distribution of piezoelectric potentials in a ZnO nanowire using the Lippman theory.[33,34] For a freestanding ZnO nanowire with strain applied along *c*-axis, the two ends of the nanowire exhibit positive and negative piezoelectric potentials, respectively (Figure 2(a)-IV). The piezoelectric potential could be as high as 0.4 V for a 600 nm nanowire as calculated.

The operation mechanism of a PENG is usually based on the piezopotential created in the piezoelectric material. Usually two electrodes are applied on the material, with the Fermi levels in

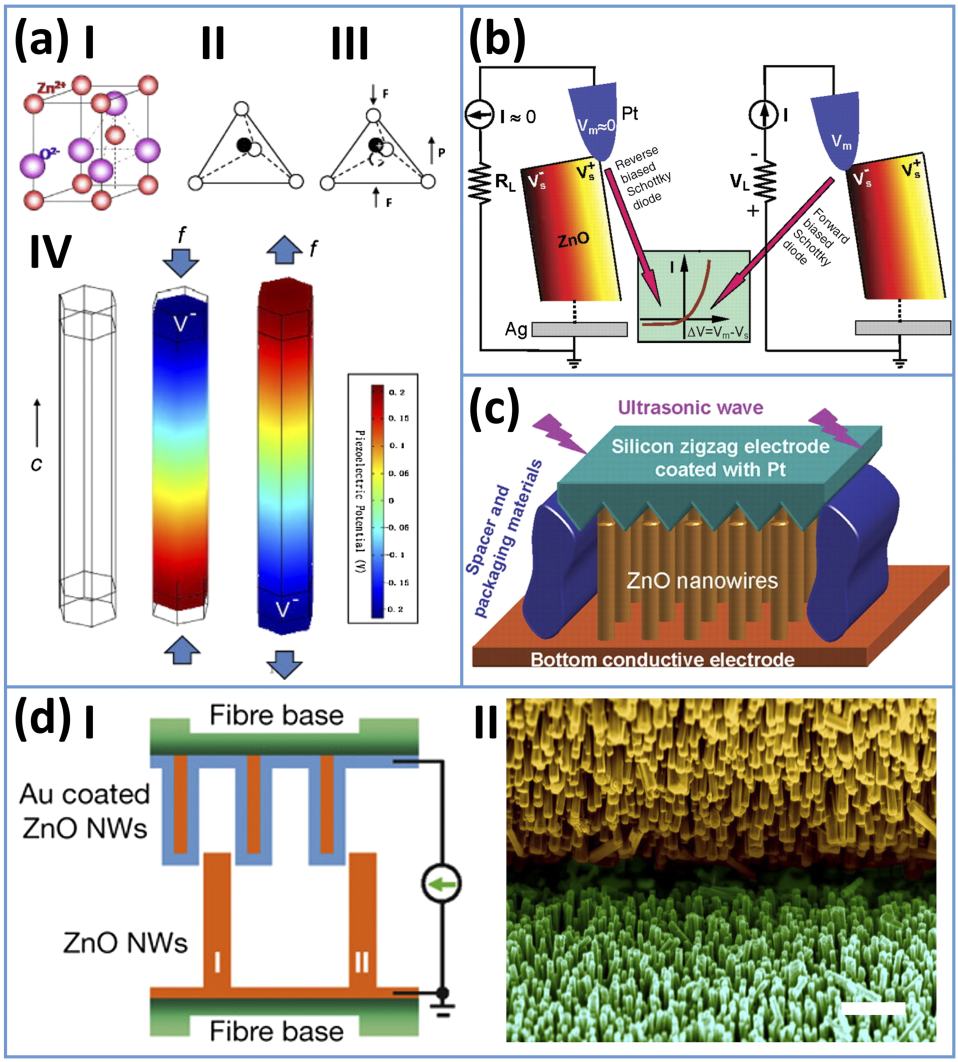

FIG. 2. The mechanism and the early studies of piezoelectric NG (PENG). (a) The mechanism of the piezopotential generation in a ZnO NW. (b) PENG as operated by AFM tip scanning above the ZnO NW array. (c) PENG as driven by ultrasonic waves. (d) Microfibre-nanowire hybrid structured PENG. The scale bar in (d)-II: 1 μm. Reproduced with permission from Z. L. Wang and J. Song, Science **312**(5771), 242 (2006). Copyright 2006 American Association for the Advancement of Science, Y. Qin, X. Wang, and Z. L. Wang, Nature **451**(7180), 809 (2008). Copyright 2008 Nature Publishing Group, Wang *et al.*, Science **316**(5821), 102 (2007). Copyright 2007 American Association for the Advancement of Science, Gao *et al.*, J. Appl. Phys. **105**(11), 113707 (2009). Copyright 2009 AIP Publishing LLC, and Z. L. Wang, Nano Today **5**(6), 540 (2010). Copyright 2010 Elsevier.[4,10,11,34,40]

the two electrodes naturally electrostatically balanced. With strains applied on the material, the created piezopotential results in differences between the internal and external Fermi levels at the contacts. To re-balance the differences in Fermi levels, the free charge carriers flow between two electrodes through external circuits, and finally a new balanced electrostatic status is achieved. Under periodical variations of the strains as triggered by mechanical forces, the PENG can produce an alternating current (AC) output. This output will be a promising power source for sustainably operating micro- or nano-systems.

PENG was first proposed based on aligned ZnO nanowire arrays, using contact-mode atomic force microscopy (AFM) with Pt-coated Si probe.[4] The Schottky barrier on the top end of the nanowire as formed by Pt and ZnO is a key for electricity generation.[35,36] While scanning above the nanowire arrays in the contact mode, the AFM probe deforms the nanowires. The stretched surface with positive potential was first contacted by the AFM probe (Figure 2(b)-left). At this time, the bias voltage of

Pt-ZnO interface is negative, and thus a reverse-biased Schottky diode is formed with little current flowing across it. When the probe contacts the compressed side of the nanowire (Figure 2(b)-right), the Pt-ZnO interface is positively biased, which introduces a sharp peak of output current, as driven by the potential difference between the two sides. The current flow finally re-balances the electrostatic status and thus the potential difference disappears. By using this method, scanning above one single ZnO nanowire generates energy of 0.05 fJ, with a voltage output of about 8 mV. However, to power a single NW device[37–39] through this method, high frequency resonance and high density NW array for high power generation are required. Further studies on advanced device designs and materials are still demanded.

To effectively couple the high-frequency ultrasonic waves for energy harvesting by PENG, a direct-current PENG is designed by our group.[11] The schematic diagram of the ultrasonic wave PENG is shown in Figure 2(c). The ZnO nanowire arrays were grown on a sapphire substrate with a ZnO buffer thin film layer as the electrode.[41,42] On the top side, a silicon substrate with a fabricated zigzag surface coated with Pt layer was applied, which operates like multiple AFM probes scanning on the ZnO nanowire arrays. The voltage and current outputs are measured with a created ultrasonic wave of about 41 kHz. The unidirectional current of about 0.15 nA is obtained, with the open-circuit voltage of only 0.7 mV. This voltage is smaller than that obtained by the AFM probe since the ZnO nanowires are less deflected by the ultrasonic waves than that by the AFM probe.[4]

To effectively harvest mechanical motion from the body movement, a microfibre–nanowire hybrid structure based PENG is designed in our group.[10] This time, the ZnO nanowire arrays are grown on the surface of microfibres, using the hydrothermal approach,[43] with pre-deposited ZnO thin film layer as the electrode. And then, half of the microfibres are coated with Au layers (group A fibre), and the others are with no further treatment (group B fibre). One group A fibre and one group B fibre are tangled together for electricity generation (Figure 2(d)-I). Here the group A fibre with nanowire structures works as the AFM probes or the zigzag electrode for triggering ZnO nanowires on the group B fibre. The SEM picture of the contact interface is shown in Figure 2(d)-II, with the faked yellow for group A fibre and green for group B fibre. Through this method, about 1-3 mV of the output voltage and 4 nA of the output current are generated, with an estimated power density of 20-80 mW/m^2 extracted from the output performance of a textile fabricated by these microfibres.

As we mentioned above, it is crucial to enhance the output performance of PENG through effective integration of nanowire arrays. The key of the integration is synchronization of the deformation of each nanowire, so that the outputs especially the voltage outputs from these nanowires can be added up. Recently, two effective integration structures have been developed from our group. One structure is the lateral-nanowire integrated NG (LING), with parallel nanowires grown or fabricated on the flexible substrates[12,13,44] (Figure 3(a)). This structure can effectively harvest strain energy during the bending deformation of the substrate. Since the diameter of the nanowires is much smaller than the thickness of the substrate, all the nanowires on the substrate are stretched or compressed simultaneously, and thus the output performance can be added up.[44] A previous report of LING, as shown in the inset of Figure 3(a), has demonstrated peak power output of 11 mW/cm^3 with effective energy conversion of 4.6%.[13] This device integration represents a potential approach for large-scale nanowire integration not only for electrical generation but also for nanowire-based electronic or optoelectronic devices. The other structure is the vertical-nanowire integrated NG (VING), with the device directly fabricated based on the grown vertical nanowire arrays[9,11,12,45] (Figure 3(b)). The ultrasonic wave driven NG and the hybrid microfibre-nanowire NG can both be categorized as this structure. This structure can effectively harvest energy from compression deformation of the NG. To enhance the voltage output, the VING can be stacked together to meet the threshold voltage required by electronic devices. 58 V as the voltage, 134 μA as the current output, and power density of 0.78 W/cm^3 were demonstrated in this type of PENG.[45] This power output has been demonstrated for wireless transmission (Figure 3(b))[9] and neuroprosthetic devices.[45]

Besides ZnO, a lot of other advanced materials have been used for PENG. A typical example is the 2D materials, such as MoS_2.[15] (Figure 3(c)-I) This MoS_2 flake based device was fabricated on the flexible substrate with metal electrodes deposited on the two sides of the flake (Figure 3(c)-II). Similar to a LING, the deformation of the substrate stretches or compresses the MoS_2 (Figure 3(c)-II inset). From a single device based on a monolayer flake with the size of about

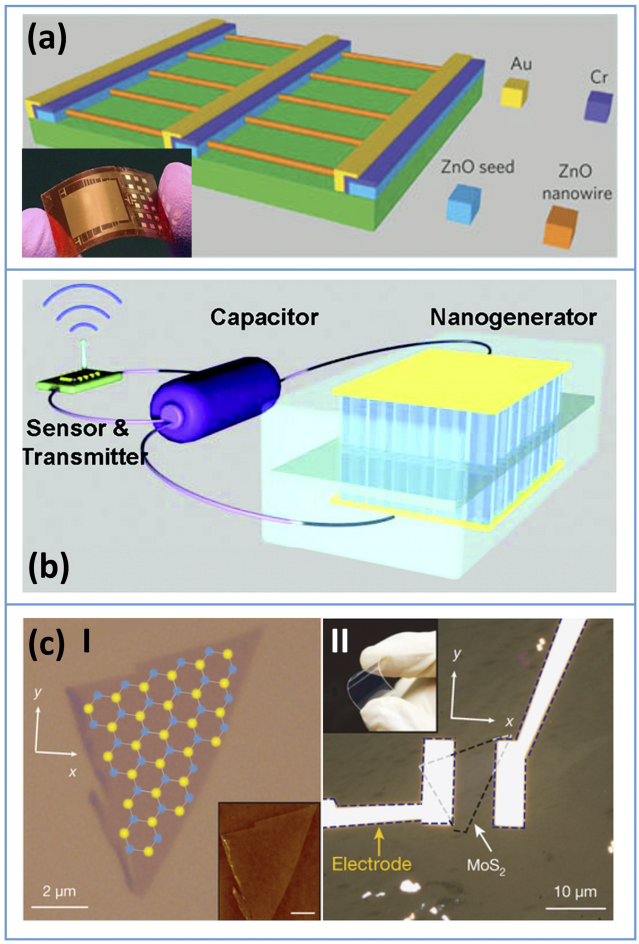

FIG. 3. Piezoelectric NGs (PENG) with novel structures and materials. (a) The structure of lateral-nanowire integrated NG (LING) and a photo of a LING in inset. (b) A vertical-nanowire integrated NG (VING) for wireless transmission. (c) The smallest NG (II) based on a MoS_2 flake (I). The inset in (II) shows the photo and that in (I) shows AFM topological profile (scale bar: 2 μm). Reproduced with permission from Hu *et al.*, Nano Lett. **11**(6), 2572 (2011). Copyright 2011 The American Chemical Society, Xu *et al.*, Nat. Nanotechnol. **5**(5), 366 (2010). Copyright 2010 Nature Publishing Group, Zhu *et al.*, Nano Lett. **10**(8), 3151 (2010). Copyright 2010 The American Chemical Society, and Wu *et al.*, Nature **514**(7523), 470 (2014). Copyright 2014 Nature Publishing Group.[9,12,13,15]

50 μm^2, an instantaneous open-circuit voltage of 18 mV and current output of 27 pA are achieved. At the matched load resistance of about 220 MΩ, the peak output power density of 2 mW/m^2 is demonstrated at the strain of 0.53%. Other typical materials used for PENG include polyvinylidene fluoride (PVDF),[17,46] barium titanate ($BaTiO_3$),[47] cadmium sulfide (CdS),[48] gallium nitride (GaN),[49,50] and so on. Studies are also conducted to develop various flexible PENGs with a wide choice of materials towards broad applications.[51–55]

With the conjugated mechanism of triboelectrification and electrostatic induction effects, TENG has been developed by our group in 2012.[2,5,18,19,56] Through the rapid growth of this new field in recent years, the fundamental modes, structures, and materials have been optimized, with a maximum area power output of 500 W/m^2[57] and energy conversion efficiency of over 50%[58,59] demonstrated (Figures 5(a) and (b)).

There have been four basic modes of TENGs with their own unique advantages, characteristics, and applications, including vertical contact-separation (CS) mode, lateral-sliding (LS) mode, single-electrode (SE) mode, and freestanding triboelectric-layer (FT) mode. For all these basic modes TENGs, there are at least one pair of triboelectric surfaces contact together initially (for FT mode, there are usually two pairs of triboelectric surfaces). And there are also at least two electrodes, which

are carefully insulated from each other. For SE mode, the ground is considered as the other electrode.[60] The distinct abilities for attracting electrons of the two triboelectric surfaces result in transfer of electrostatic charges from one surface to the other surface. When a displacement is applied on one triboelectric layer, the movement of the electrostatic charges breaks the original electrostatic status, and then the potential difference is built between the two electrodes. The current through the external load is driven by such potential difference to balance the electrostatic status. The reverse-direction movement of the triboelectric layer induces the inverse potential difference between electrodes, and hence the opposite direction of the current flow. Therefore, under periodical mechanical triggering, an AC output can be obtained by the TENG, and its operations are characterized by the voltage V between electrodes, charge transfer Q between electrodes, and relative displacement x between triboelectric layers.

The CS mode TENG is triggered by the contact and separation process of the two triboelectric layers[61–63] (Figure 4(a)). The electrodes are attached on the back sides of the triboelectric layers. As the most basic and the firstly developed one, this mode holds advantages of simple structure, facile fabrication, robustness, and high peak output current. The structural figure-of-merit (FOM) is relatively higher than that of sliding based structures.[56] The output performance can be enhanced by stacked multilayer structures.[64,65] The major disadvantage is the difficulty in packaging strategy due to its varied volume.

The LS mode TENG is triggered by relative sliding between triboelectric layers.[66,67] (Figure 4(b)) Similar to the CS mode TENG, the electrodes are also attached on the back sides of the triboelectric layers. The long displacement during sliding process in this mode results in the lower structural FOM as compared with CS mode.[56] However, the charge generation is more effective than that by merely contact, with higher charge density created.[66] A crucial advantage of this mode TENG is that the current output performance can be greatly improved through grating structures.[57,59,67] The grating sliding structured LS mode TENG can also be altered to be rotational grating[68,69] or cylindrical grating[70] structures.

Both CS and LS modes TENGs suffer from a common disadvantage that the moving triboelectric layer with the back electrode should have a wire connected. Such a configuration might limit the applications of TENG in a broader area for energy harvesting from free-moving objectives. To solve this issue, we may simply remove one back electrode to form a SE mode TENG[71,72] (Figure 4(c)).

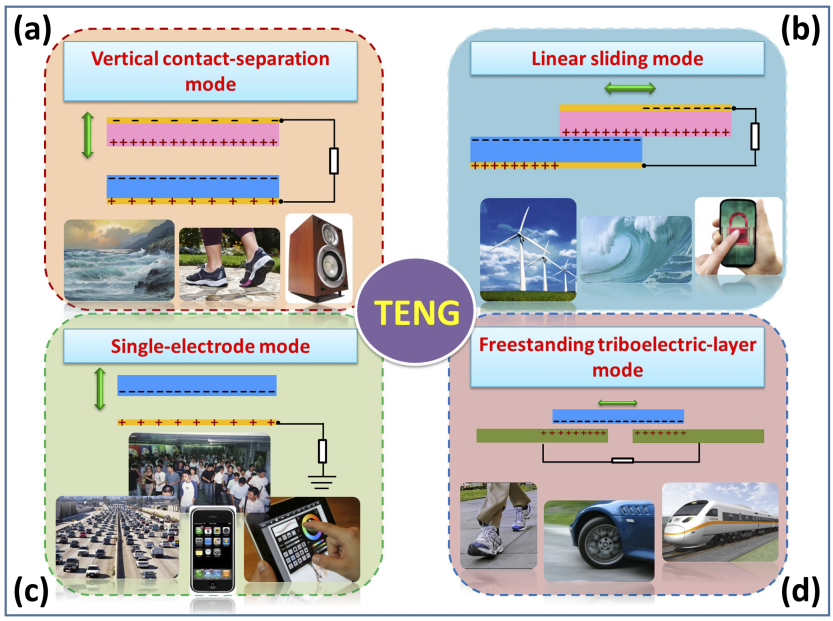

FIG. 4. Four basic operation modes for TENG. (a) Vertical contact-separation (CS) mode; (b) in-plane lateral sliding (LS) mode; (c) single electrode (SE) mode; (d) freestanding triboelectric-layer (FT) mode. Reproduced with permission from Z. L. Wang, Faraday Discuss. **176**, 447–458 (2015). Copyright 2015 The Royal Society of Chemistry.[18]

This mode of TENG holds the simplest structure, and it is very easy to fabricate. However, the output performance of this mode is greatly limited by the small charge transfer amount and the limited voltage.[60] The application of this mode TENG is mostly for self-powered sensing devices.[71,72]

FT mode TENG can be operated with a triboelectric layer moving freely between the two static electrodes[60,73] (Figure 4(d)). In this mode, the moving triboelectric layer without attached electrode can move with or without contact with two static electrodes, and hence it is extraordinarily robust.[73,74] At the same time, the high output performance is demonstrated, with the high structural FOM achieved.[56] Based on the advantages of high output, facile fabrication, and integration, this mode has been demonstrated for various high output TENGs with records in both the maximum power output and energy conversion efficiency.[57,59,69]

The theoretical studies of operations, output performances, and simulation results of TENG with all the four TENG modes have been reported by our group.[60,75–78] Based on the theories, the figure-of-merit (FOM) for quantifying the output performance of TENG has been defined as its standard. This FOM includes two parts: the structural FOM is proposed to characterize the structure designs/modes of the TENG, and the materials FOM, which equals to the square of the surface charge density, works as the standard for quantifying triboelectric properties of materials/surfaces.[56] Therefore, the optimization of the TENG has been conducted in the both aspects of structures and materials. To enhance the output of TENG through structural optimization, the multi-layer integrations[26,64] and grating structures[59,67,69,79] have been developed. The surface triboelectric charge density created in materials can be quantitatively measured through AFM[80,81] and by using liquid metals,[56,58] and then it can be enhanced through advanced materials and surfaces,[63,82–85] ionized air injection,[86] and surface functionalization.[87,88]

All kinds of mechanical energies that are available in our daily life, such as human motions, vibrations, wind, flowing water, and others, can be harvested by TENG.[19,89] The high output voltage achieved by TENG can be directly utilized for applications which require high onset voltage.[90] TENG can also be integrated with energy storage units (battery or supercapacitor) to form a self-charging power system (SCPS) for energy harvesting and storage simultaneously, with usually a full-wave bridge rectifier to convert the AC output to be direct current (DC) signals[91–93](Figure 5(c)). However, such a direct connection results in low energy conversion efficiency, as reflected by the quickly decayed charging rate during charging a capacitor, and the limited saturation voltage. Such a low energy storage efficiency greatly limits the overall efficiency during energy utilization in the SCPS. Our group has demonstrated two effective strategies to address this issue.

The first strategy we have developed is the designed charging cycles for achieving effective energy storage.[94] Previously through the direct charging cycles with the direct connection of the TENG and the energy storage units as described above, the charging rate decays quickly, the maximum energy storage efficiency is 25%, and the saturation voltage is less than the half of the open-circuit voltage. Through the designed charging cycles as enabled by the automatically triggered switch, the charging rate decays slower, the energy storage efficiency becomes up to 50%, and the saturation voltage is up to the open-circuit voltage. Through this designed charging cycle, in some cases, the output power could be promoted by several times, as demonstrated through powering a commercially available calculator. Such an effective energy storage strategy enabled the possibility to build SCPS with high power output and high overall energy efficiency.

The other strategy is through integration with a power-management unit (PMU) to manage the power output characteristics of TENG, through various components such as a transformer,[95] an electronic circuit with a coupled inductor as controlled by electronic logic-control switches,[96] and capacitors with automatic switched connections.[97] For example, the PMU as developed by Niu *et al.* has demonstrated 50%-60% in overall energy conversion efficiency and DC average power output of over 1 mW.[96] This PMU is through a coupled inductor with control switches triggered by logic control circuits. The power output has been applied to drive various electronic devices for health monitoring, environmental monitoring, scientific computing, and wireless communication (Figure 5(d)). Such studies on PMU will greatly broaden the applications of TENG to fit more devices with distinct equivalent impedances.

Here we would like to emphasise a crucial potential application of TENG: harvesting low-frequency wave energy in ocean, as a rich resource for large scale clean energy generation.[2,18,21–24]

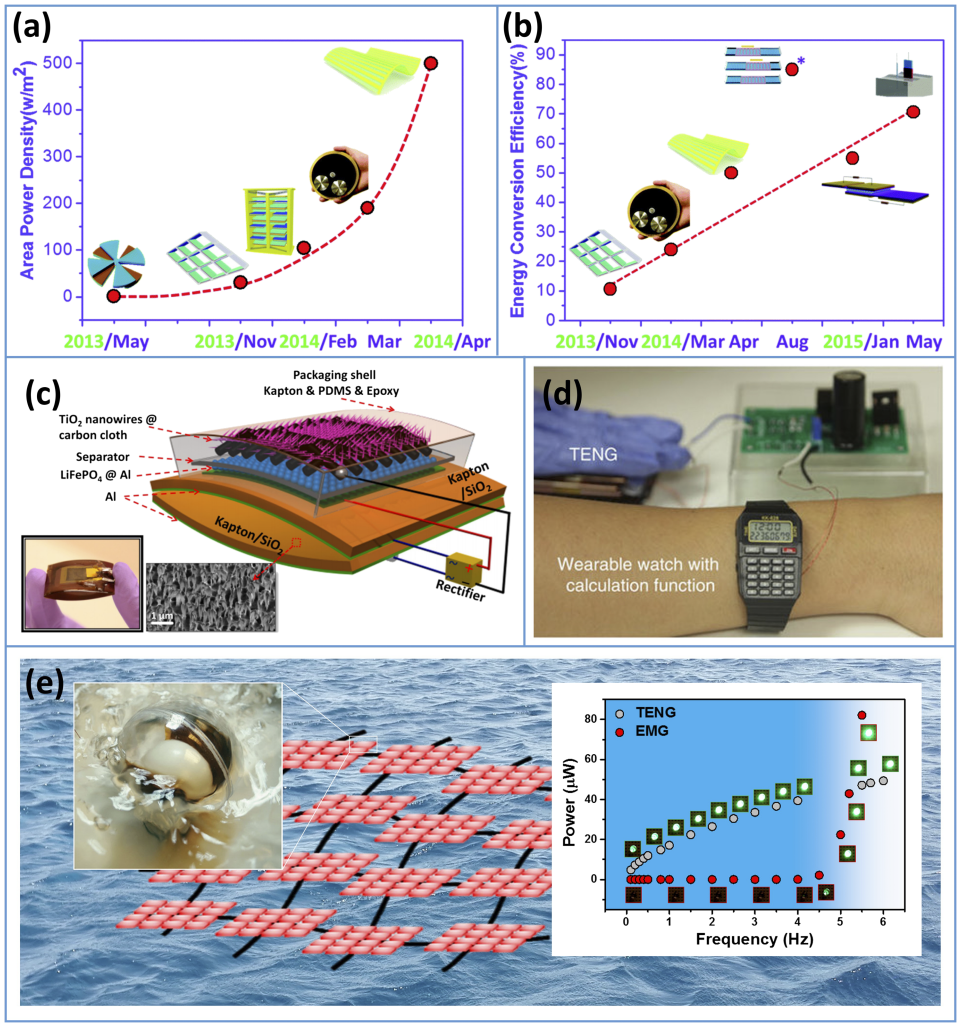

FIG. 5. The rapid development of triboelectric NG (TENG). ((a) and (b)) The rapid enhancement of (a) the area power density and (b) energy conversion efficiency. (c) A packaged self-charging power system including a TENG and a flexible battery. The insets show the picture and the nanowire structure in the triboelectric surface. (d) A watch as powered by a self-charging power system with a power-management unit. (e) The proposed TENG-network idea for large scale blue energy harvesting. The left inset shows a single unit of TENG. The right inset shows pictures of a light-emitting diode (LED) bulb and the power as powered by TENG and electromagnetic generator (EMG) in low frequency. Reproduced with permission from Zi *et al.*, ACS Nano **10**(4), 4797 (2016). Copyright 2016 The American Chemical Society, Z. L. Wang, J. Chen, and L. Lin, Energy Environ. Sci., **8**, 2250 (2015). Copyright 2015 The Royal Society of Chemistry, Chen *et al.*, ACS Nano **9**(3), 3324 (2015). Copyright 2015 The American Chemical Society, Wang *et al.*, ACS Nano **7**(12), 11263 (2013). Copyright 2013 The American Chemical Society, and Niu *et al.*, Nat. Commun. **6**, 8975 (2015). Copyright 2015 Nature Publishing Group.[3,19,21,91,96]

Our proposed approach is by integration of single TENG units (as shown in the left inset of Figure 5(e)) to be a TENG network (TENG-NW) through cables, and the output signals from TENG units can be added together for high power output. There are two advantages for this approach for wave energy harvesting. First, considering that the waves are randomly oscillated, such an approach through multiple TENG units can "catch" ocean waves effectively for efficient energy harvesting. Second, considering the abundance of the low-frequency energy in the ocean waves, tides, and streams, and that TENG is a potential "killer application" to harvest sub-3 Hz low frequency mechanical energy, TENGs are more suitable and efficient than traditional EMGs for low-frequency energy harvesting[3] (Figure 5(e), right inset). Through this approach, we predicted that the average power density output of 1.15 MW/km^2 can be achieved, with low cost.[21] Therefore, TENG is highly possible to be developed as the next-generation large scale energy harvesting technology, considering the abundance of the energy in the ocean waves—the blue energy.

The invention of the TENG opens new possibilities for developing related areas, as a distinctly different energy technology. Recently, a roadmap has been proposed for further development of TENG.[18] Our efforts on studying TENG have already initiated world-wide research with continuously growing impact. Commercialization of the TENG technology can also be expected very soon.

Thermal energy is another abundant energy in the environment. Thermoelectric energy harvester has been developed to harvest thermal energy with a spatial temperature gradient, through the Seebeck effect. To efficiently harvest the thermal energy, the required temperature gradient is usually high, which is not easy to be satisfied in our daily life. Besides, the materials for thermoelectric energy harvesters are usually expensive.[98] Alternatively, it is possible to use the pyroelectric materials for thermal energy harvesting from the temperature variations with respect to the time. Our group has developed pyroelectric NG (PyENG) in 2012 for thermal energy harvesting.[6] The energy harvested by the PyENG has been demonstrated for powering small electronics.

To characterize the ability of a pyroelectric material for converting thermal energy into electricity, the key parameter is the pyroelectric coefficient, which is related to the changing rate of the polarization density with respect to the temperature. This pyroelectric coefficient is contributed by two parts, and the relative magnitudes of them vary for different materials.[99–101] The primary part of the pyroelectric coefficient is related to the variation of the dipole moments with the change of the temperature. The physical nature of the varied dipole moments is explained by oscillation phenomena of the atoms/ions in different temperatures.[14,102,103] The secondary part of the coefficient is due to the piezoelectric effect as induced by thermal expansion in the crystal.

The mechanism of electric generation based on the primary pyroelectric coefficient is illustrated by taking $KNbO_3$ NW PyENG as an example.[102] In this material, the dipole moments as well as the spontaneous polarization density has already existed in the crystal (Figure 6(a)-I). With the increased temperature, there are higher degree random oscillations in the ions, resulting in smaller effective dipole moments and hence the polarization density.[104] To rebalance the electrostatic status brought by the decreased polarization density, free electrons flow from the top electrode to the bottom electrode through the external load (Figure 6(a)-II). Once the device is cooled down, the ions oscillate less and the dipole moments are recovered. And then the increased polarization density induced charge flows in the reversed direction (Figure 6(a)-III). The operation of the PyENG can also be driven by the primary and the secondary pyroelectric effects at the same time.[46]

The first PyENG is fabricated based on ZnO nanowire arrays[6] (Figure 6(b)). The pyroelectric current and voltage coefficients for the 200 nm diameter ZnO nanowire arrays are estimated as about 1.2-1.5 nC/(cm^2 K) and 2.5-4.0 $\times$ 10^4 V/mK, respectively. And then, another type of PyENG is reported by us based on the $KNbO_3$ nanowire and polydimethylsiloxane (PDMS) polymer composite, with the pyroelectric coefficient demonstrated as around 0.8 nC/(cm^2 K)[102] (Figure 6(c)). The output voltage and current can achieve 2.5 mV and 25 pA, respectively, under thermal energy created by the solar irradiation. $Pb(Zr_xTi_{1-x})O_3$ (PZT) film was also used to demonstrate PyENG, with the high output performance due to its high pyroelectric coefficient[105] (Figure 6(d)). With the high output performance with voltage of about 22 V and current of about 171 nA/cm^2, the PyENG can be utilized to drive a liquid-crystal display (LCD), a light-emitting diode (LED), and a wireless sensor. For broader applications, Lee *et al.* also demonstrated a highly stretchable piezoelectric-pyroelectric nanogenerator with using a micro-patterned polymer polyvinylidene fluoride–trifluoroethylene [P(VDF-TrFE)] copolymer, PDMS–carbon nanotube (CNT) composite, and graphene nanosheets[14] (Figure 6(e)). Recently, the PVDF materials are also fabricated as PyENGs for harvesting thermal energies from hot water,[103] frictional heat,[46] and other circumstances, with broad potential applications for medical diagnostic devices, environmental monitors, personal electronics, etc.

As we discussed above, thermal energy can also be harvested based on the Seebeck effect when there is temperature gradient existing in the environment. Such a gradient possibly exists between human body and ambient environment. Therefore, it is possible to fabricate the thermoelectric nanogenerator (ThENG) as a wearable energy harvester to power devices for human-machine interface. Our group has conducted several studies on this type of NG. Our first ThENG is fabricated based on a single Sb-doped nanobelt[7] (Figures 7(a)-I and 7(a)-III). The temperature gradient in the nanobelt (as simulated in Figure 7(a)-II) can produce outputs of 10 mV in the voltage and 194 nA in the current, respectively. As calculated, the Seebeck coefficient can achieve 350 μV/K with a power factor of

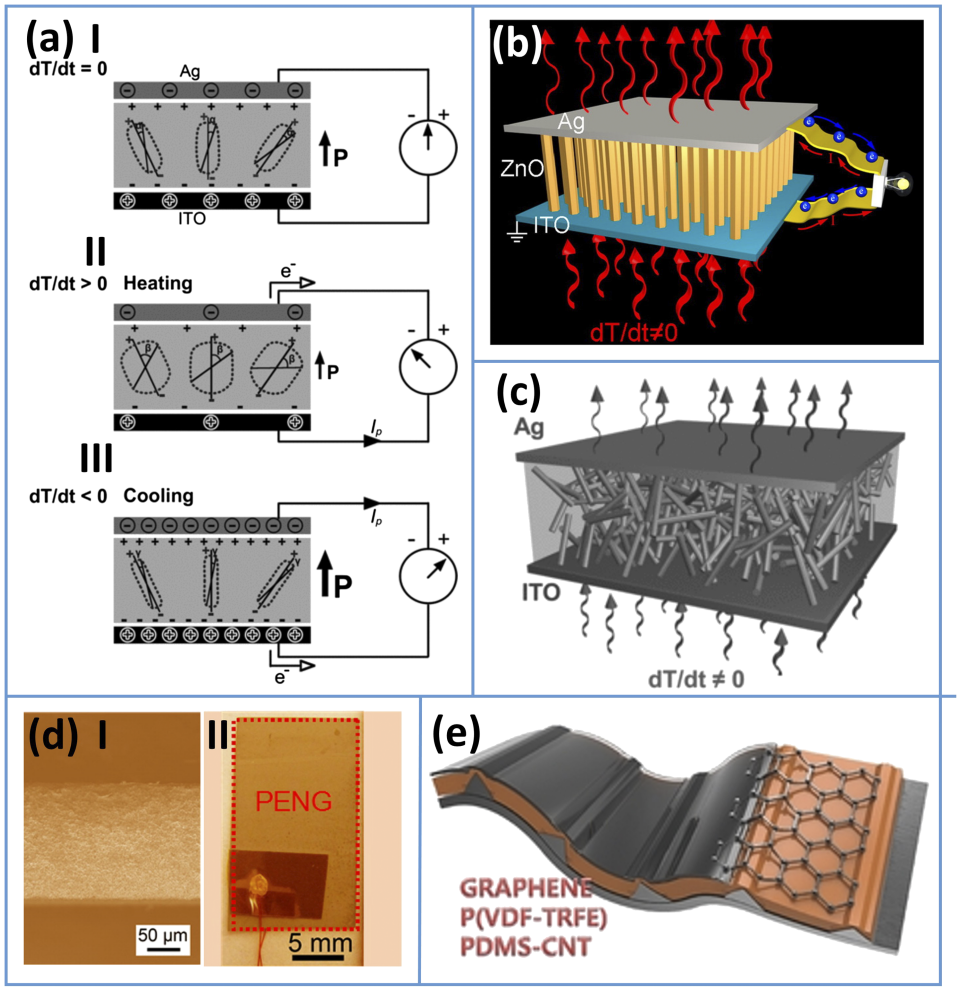

FIG. 6. Mechanism and representative studies of PyENG. (a) The mechanism of a $KNbO_3$ NW PyENG based on the first pyroelectric effect. (b) PyENG based on ZnO NW arrays. (c) PyENG based on $KNbO_3$ NWs. (d) PyENG based on $Pb(Zr_xTi_{1-x})O_3$ (PZT) film. (e) Highly stretchable piezoelectric-pyroelectric NG. Reproduced with permission from Yang *et al.*, Nano Lett. **12**(6), 2833 (2012). Copyright 2012 The American Chemical Society, Lee *et al.*, Adv. Mater. **26**(5), 765 (2014). Copyright 2014 The Wiley, Yang *et al.*, Adv. Mater. **24**(39), 5357 (2012). Copyright 2012 The Wiley, and Yang *et al.*, Nano Lett. **12**(12), 6408 (2012). Copyright 2012 The American Chemical Society.[6,14,102,105]

3.2×10^{-4} W/(mK^2). And then, based on the composite consisting of Te NWs (Figure 7(b)-II) and poly(3-hexylthiophene-2,5-diyl) (P3HT) polymer, a flexible ThENG (Figure 7(b)-I) is demonstrated, with the Seebeck coefficient as about 285 μV/K.[106] It can also be demonstrated as a self-powered temperature sensor.

The energy in the fluid has been focused for a long time. Previously, towards blue energy harvesting, our group has demonstrated TENGs for mechanical energy harvesting from fluids.[21,23,24] However, this method is mainly targeted at energy harvesting from large-scale water flows. We also explored other approaches for harvesting flow energy, especially from micro-fluid. Here a new type of micro-fluid nanogenerator (MFG), with the mechanism based on ion streams, is briefly introduced[8] (Figure 7(c)).

As shown in Figure 7(c)-I, the micro-fluid is usually an ionic fluid such as the KCl solution, and the micro-channels are made of PDMS. To enhance the effective inner surface area, the PDMS channel is made using a template with patterns on it. Inlet and outlet openings are made at the two ends of the patterned channel for ion flows, respectively. The electrodes are attached on the both openings for electrical output. The fluid is injected and the flow rate is controlled by a syringe. As we know the PDMS surface has trend to be negatively charged,[56] thus the positive ions (such as K^+ ions in the KCl

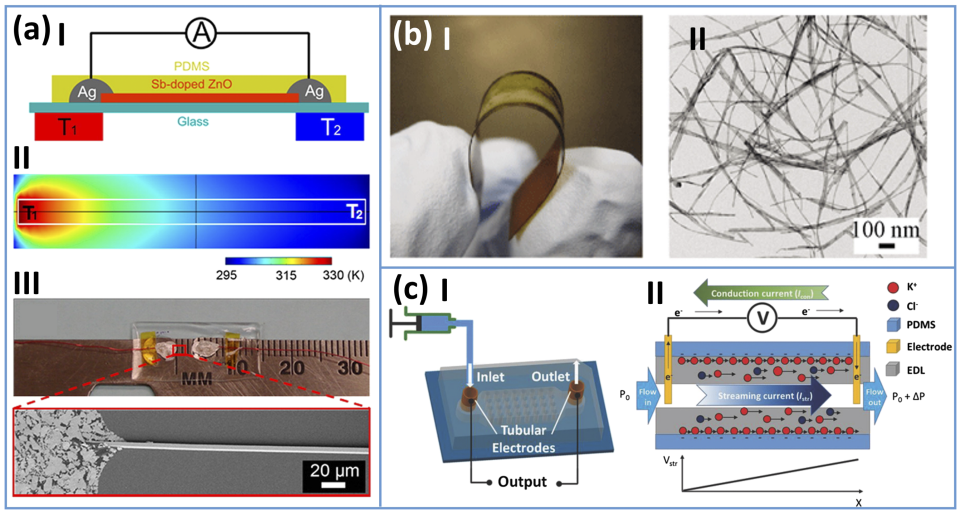

FIG. 7. Other types of nanogenerators. (a) The schematic diagram (I), the simulated temperature gradient (II), and photo/SEM picture (III) of a Sb-doped ZnO NW ThENG; (b) the photo of a flexible ThENG (I), composed of Te NW (II) and poly(3-hexylthiophene-2,5-diyl) (P3HT) polymer. (c) The schematic diagram (I) and mechanism (II) of a micro-fluid nanogenerator. Reproduced with permission from Yang *et al.*, ACS Nano **6**(8), 6984 (2012). Copyright 2012 The American Chemical Society, Zhang *et al.*, Adv. Mater. **27**(41), 6482 (2015). Copyright 2015 Wiley, and Yang *et al.*, Nano Res. **5**(12), 888 (2012). Copyright 2015 Springer.[7,8,106]

solution) flowing through the channel is likely to be attracted in the negative charged PDMS surface, and the electric double layers (EDL) are formed. Therefore, the ion flow transported in the EDL regions mainly carries positive charges, resulting the potential difference between the upstream positions and the downstream positions.[107,108] This potential difference is reflected by the voltage across the electrodes, which drives the current flow through the external circuit (Figure 7(c)-II). Through this mechanism, 1.75 nA of the output current is produced and a nanowire based pH sensor is powered by the MFG. This MFG with small size is easy to be fabricated through lithography technology and will become an irreplaceable part in the micro-fluid systems, for driving lab-on-chip systems with broad applications.

The development of the electronic devices follows the trends of minimization, functionality, portability, and now towards self-powerbility.[109] The invention of the NGs brings us the possibility to let the electronic systems powered by the energy harvested from ambient environment, which is essential for the development of the IoT. In this paper, we reviewed the development of the nanogenerators in the past decade. NG is first developed as PENG based on the piezoelectric effect, with a large quantity of novel integrations and materials being developed for continuously enhanced output performance. Through the coupled contact electrification and electrostatic induction effects, TENG has exhibited its unique characteristics and high output performance for efficient mechanical energy harvesting, which will potentially make huge impacts in broad application areas. Both PENG and TENG have already attracted worldwide attentions on research and possible commercialization. We also developed PyENG and ThENG for harvesting thermal energy from the environment. The novel NGs such as that based on ion streams are also explored. The rapid development of the NG family will set the foundation for self-powered systems and possibly drive the development of the energy and sensing technologies in future.

This work was supported by the Hightower Chair foundation and the "thousands talents" program for pioneer researcher and his innovation team, China.

The authors declare no competing financial interests.

[1] Z. L. Wang, Sci. Am. **298**(1), 82 (2008).
[2] Z. L. Wang, ACS Nano **7**(11), 9533 (2013).
[3] Y. Zi, H. Guo, Z. Wen, M.-H. Yeh, C. Hu, and Z. L. Wang, ACS Nano **10**(4), 4797 (2016).
[4] Z. L. Wang and J. Song, Science **312**(5771), 242 (2006).

[5] F.-R. Fan, Z.-Q. Tian, and Z. L. Wang, Nano Energy **1**(2), 328 (2012).
[6] Y. Yang, W. Guo, K. C. Pradel, G. Zhu, Y. Zhou, Y. Zhang, Y. Hu, L. Lin, and Z. L. Wang, Nano Lett. **12**(6), 2833 (2012).
[7] Y. Yang, K. C. Pradel, Q. Jing, J. M. Wu, F. Zhang, Y. Zhou, Y. Zhang, and Z. L. Wang, ACS Nano **6**(8), 6984 (2012).
[8] R. Zhang, S. Wang, M.-H. Yeh, C. Pan, L. Lin, R. Yu, Y. Zhang, L. Zheng, Z. Jiao, and Z. L. Wang, Adv. Mater. **27**(41), 6482 (2015).
[9] Y. Hu, Y. Zhang, C. Xu, L. Lin, R. L. Snyder, and Z. L. Wang, Nano Lett. **11**(6), 2572 (2011).
[10] Y. Qin, X. Wang, and Z. L. Wang, Nature **451**(7180), 809 (2008).
[11] X. Wang, J. Song, J. Liu, and Z. L. Wang, Science **316**(5821), 102 (2007).
[12] S. Xu, Y. Qin, C. Xu, Y. Wei, R. Yang, and Z. L. Wang, Nat. Nanotechnol. **5**(5), 366 (2010).
[13] G. Zhu, R. Yang, S. Wang, and Z. L. Wang, Nano Lett. **10**(8), 3151 (2010).
[14] J.-H. Lee, K. Y. Lee, M. K. Gupta, T. Y. Kim, D.-Y. Lee, J. Oh, C. Ryu, W. J. Yoo, C.-Y. Kang, S.-J. Yoon, J.-B. Yoo, and S.-W. Kim, Adv. Mater. **26**(5), 765 (2014).
[15] W. Wu, L. Wang, Y. Li, F. Zhang, L. Lin, S. Niu, D. Chenet, X. Zhang, Y. Hao, and T. F. Heinz, Nature **514**(7523), 470 (2014).
[16] H. B. Kang, J. Chang, K. Koh, L. Lin, and Y. S. Cho, ACS Appl. Mater. Interfaces **6**(13), 10576 (2014).
[17] C. Chang, V. H. Tran, J. Wang, Y.-K. Fuh, and L. Lin, Nano Lett. **10**(2), 726 (2010).
[18] Z. L. Wang, Faraday Discuss. **176**, 447–458 (2015).
[19] Z. L. Wang, J. Chen, and L. Lin, Energy Environ. Sci. **8**, 2250 (2015).
[20] Z. L. Wang, L. Lin, J. Chen, S. Niu, and Y. Zi, *Triboelectric Nanogenerators* (Springer International Publishing, 2016), ISBN: 3319400398, 9783319400396.
[21] J. Chen, J. Yang, Z. Li, X. Fan, Y. Zi, Q. Jing, H. Guo, Z. Wen, K. C. Pradel, S. Niu, and Z. L. Wang, ACS Nano **9**(3), 3324 (2015).
[22] H. Guo, Z. Wen, Y. Zi, M.-H. Yeh, J. Wang, L. Zhu, C. Hu, and Z. L. Wang, Adv. Energy Mater. **6**, 1501593 (2015).
[23] X. Wang, S. Niu, Y. Yin, F. Yi, Z. You, and Z. L. Wang, Adv. Energy Mater. **5**(24), 1501467 (2015).
[24] Z. Wen, H. Guo, Y. Zi, M.-H. Yeh, X. Wang, J. Deng, J. Wang, S. Li, C. Hu, L. Zhu, and Z. L. Wang, ACS Nano **10**(7), 6526 (2016).
[25] X. Pu, L. Li, H. Song, C. Du, Z. Zhao, C. Jiang, G. Cao, W. Hu, and Z. L. Wang, Adv. Mater. **27**(15), 2472 (2015).
[26] W. Yang, J. Chen, G. Zhu, J. Yang, P. Bai, Y. Su, Q. Jing, X. Cao, and Z. L. Wang, ACS Nano **7**(12), 11317 (2013).
[27] F. Yi, X. Wang, S. Niu, S. Li, Y. Yin, K. Dai, G. Zhang, L. Lin, Z. Wen, H. Guo, J. Wang, M.-H. Yeh, Y. Zi, Q. Liao, Z. You, Y. Zhang, and Z. L. Wang, Sci. Adv. **2**(6), e1501624 (2016).
[28] J. Chen, G. Zhu, W. Yang, Q. Jing, P. Bai, Y. Yang, T.-C. Hou, and Z. L. Wang, Adv. Mater. **25**(42), 6094 (2013).
[29] J. Yang, J. Chen, Y. Yang, H. Zhang, W. Yang, P. Bai, Y. Su, and Z. L. Wang, Adv. Energy Mater. **4**(6), 1301322 (2014).
[30] Y. Yang, G. Zhu, H. Zhang, J. Chen, X. Zhong, Z.-H. Lin, Y. Su, P. Bai, X. Wen, and Z. L. Wang, ACS Nano **7**(10), 9461 (2013).
[31] S. Wang, X. Mu, X. Wang, A. Y. Gu, Z. L. Wang, and Y. Yang, ACS Nano **9**(10), 9554 (2015).
[32] Z. L. Wang, Adv. Mater. **19**(6), 889 (2007).
[33] Y. Gao and Z. L. Wang, Nano Lett. **7**(8), 2499 (2007).
[34] Z. Gao, J. Zhou, Y. Gu, P. Fei, Y. Hao, G. Bao, and Z. L. Wang, J. Appl. Phys. **105**(11), 113707 (2009).
[35] R. F. Pierret, *Semiconductor Device Fundamentals* (Pearson Education, 1996).
[36] W. I. Park, G.-C. Yi, J.-W. Kim, and S.-M. Park, Appl. Phys. Lett. **82**(24), 4358 (2003).
[37] Y. Huang, X. Duan, Y. Cui, L. J. Lauhon, K.-H. Kim, and C. M. Lieber, Science **294**(5545), 1313 (2001).
[38] A. Bachtold, P. Hadley, T. Nakanishi, and C. Dekker, Science **294**(5545), 1317 (2001).
[39] J. Chen, V. Perebeinos, M. Freitag, J. Tsang, Q. Fu, J. Liu, and P. Avouris, Science **310**(5751), 1171 (2005).
[40] Z. L. Wang, Nano Today **5**(6), 540 (2010).
[41] X. Wang, J. Song, P. Li, J. H. Ryou, R. D. Dupuis, C. J. Summers, and Z. L. Wang, J. Am. Chem. Soc. **127**(21), 7920 (2005).
[42] X. Wang, C. J. Summers, and Z. L. Wang, Nano Lett. **4**(3), 423 (2004).
[43] J. W. P. Hsu, Z. R. Tian, N. C. Simmons, C. M. Matzke, J. A. Voigt, and J. Liu, Nano Lett. **5**(1), 83 (2005).
[44] R. Yang, Y. Qin, L. Dai, and Z. L. Wang, Nat. Nanotechnol. **4**(1), 34 (2009).
[45] G. Zhu, A. C. Wang, Y. Liu, Y. Zhou, and Z. L. Wang, Nano Lett. **12**(6), 3086 (2012).
[46] Y. Zi, L. Lin, J. Wang, S. Wang, J. Chen, X. Fan, P.-K. Yang, F. Yi, and Z. L. Wang, Adv. Mater. **27**(14), 2340 (2015).
[47] Z. Wang, J. Hu, A. P. Suryavanshi, K. Yum, and M.-F. Yu, Nano Lett. **7**(10), 2966 (2007).
[48] Y.-F. Lin, J. Song, Y. Ding, S.-Y. Lu, and Z. L. Wang, Appl. Phys. Lett. **92**(2), 022105 (2008).
[49] C.-Y. Chen, G. Zhu, Y. Hu, J.-W. Yu, J. Song, K.-Y. Cheng, L.-H. Peng, L.-J. Chou, and Z. L. Wang, ACS Nano **6**(6), 5687 (2012).
[50] C.-T. Huang, J. Song, W.-F. Lee, Y. Ding, Z. Gao, Y. Hao, L.-J. Chen, and Z. L. Wang, J. Am. Chem. Soc. **132**(13), 4766 (2010).
[51] G.-T. Hwang, V. Annapureddy, J. H. Han, D. J. Joe, C. Baek, D. Y. Park, D. H. Kim, J. H. Park, C. K. Jeong, K.-I. Park, J.-J. Choi, D. K. Kim, J. Ryu, and K. J. Lee, Adv. Energy Mater. **6**(13), (2016).
[52] C. K. Jeong, S. B. Cho, J. H. Han, D. Y. Park, S. Yang, K.-I. Park, J. Ryu, H. Sohn, Y.-C. Chung, and K. J. Lee, Nano Res. **10**(2), 437 (2017).
[53] C. K. Jeong, I. Kim, K.-I. Park, M. H. Oh, H. Paik, G.-T. Hwang, K. No, Y. S. Nam, and K. J. Lee, ACS Nano **7**(12), 11016 (2013).
[54] G.-T. Hwang, J. Yang, S. H. Yang, H.-Y. Lee, M. Lee, D. Y. Park, J. H. Han, S. J. Lee, C. K. Jeong, J. Kim, K.-I. Park, and K. J. Lee, Adv. Energy Mater. **5**(10), (2015).
[55] D. R. Patil, Y. Zhou, J.-E. Kang, N. Sharpes, D.-Y. Jeong, Y.-D. Kim, K. H. Kim, S. Priya, and J. Ryu, APL Mater. **2**(4), 046102 (2014).
[56] Y. Zi, S. Niu, J. Wang, Z. Wen, W. Tang, and Z. L. Wang, Nat. Commun. **6**, 8376 (2015).
[57] G. Zhu, Y. S. Zhou, P. Bai, X. S. Meng, Q. Jing, J. Chen, and Z. L. Wang, Adv. Mater. **26**(23), 3788 (2014).

[58] W. Tang, T. Jiang, F. R. Fan, A. F. Yu, C. Zhang, X. Cao, and Z. L. Wang, Adv. Funct. Mater. **25**(24), 3718 (2015).
[59] Y. Xie, S. Wang, S. Niu, L. Lin, Q. Jing, J. Yang, Z. Wu, and Z. L. Wang, Adv. Mater. **26**(38), 6599 (2014).
[60] S. Wang, S. Niu, J. Yang, L. Lin, and Z. L. Wang, ACS Nano **8**(12), 12004 (2014).
[61] F.-R. Fan, L. Lin, G. Zhu, W. Wu, R. Zhang, and Z. L. Wang, Nano Lett. **12**(6), 3109 (2012).
[62] S. Wang, L. Lin, and Z. L. Wang, Nano Lett. **12**(12), 6339 (2012).
[63] G. Zhu, C. Pan, W. Guo, C.-Y. Chen, Y. Zhou, R. Yu, and Z. L. Wang, Nano Lett. **12**(9), 4960 (2012).
[64] P. Bai, G. Zhu, Z.-H. Lin, Q. Jing, J. Chen, G. Zhang, J. Ma, and Z. L. Wang, ACS Nano **7**(4), 3713 (2013).
[65] G. Zhu, P. Bai, J. Chen, and Z. L. Wang, Nano Energy **2**(5), 688 (2013).
[66] S. Wang, L. Lin, Y. Xie, Q. Jing, S. Niu, and Z. L. Wang, Nano Lett. **13**(5), 2226 (2013).
[67] G. Zhu, J. Chen, Y. Liu, P. Bai, Y. S. Zhou, Q. Jing, C. Pan, and Z. L. Wang, Nano Lett. **13**(5), 2282 (2013).
[68] L. Lin, S. Wang, Y. Xie, Q. Jing, S. Niu, Y. Hu, and Z. L. Wang, Nano Lett. **13**(6), 2916 (2013).
[69] G. Zhu, J. Chen, T. Zhang, Q. Jing, and Z. L. Wang, Nat. Commun. **5**, 3426 (2014).
[70] P. Bai, G. Zhu, Y. Liu, J. Chen, Q. Jing, W. Yang, J. Ma, G. Zhang, and Z. L. Wang, ACS Nano **7**(7), 6361 (2013).
[71] Y. Yang, H. Zhang, J. Chen, Q. Jing, Y. S. Zhou, X. Wen, and Z. L. Wang, ACS Nano **7**(8), 7342 (2013).
[72] Y. Yang, Y. S. Zhou, H. Zhang, Y. Liu, S. Lee, and Z. L. Wang, Adv. Mater. **25**(45), 6594 (2013).
[73] S. Wang, Y. Xie, S. Niu, L. Lin, and Z. L. Wang, Adv. Mater. **26**(18), 2818 (2014).
[74] S. Li, S. Wang, Y. Zi, Z. Wen, L. Lin, G. Zhang, and Z. L. Wang, ACS Nano **9**(7), 7479 (2015).
[75] S. Niu, Y. Liu, X. Chen, S. Wang, Y. S. Zhou, L. Lin, Y. Xie, and Z. L. Wang, Nano Energy **12**, 760 (2015).
[76] S. Niu, Y. Liu, S. Wang, L. Lin, Y. S. Zhou, Y. Hu, and Z. L. Wang, Adv. Mater. **25**(43), 6184 (2013).
[77] S. Niu, Y. Liu, Y. S. Zhou, S. Wang, L. Lin, and Z. L. Wang, IEEE Trans. Electron Devices **62**(2), 641 (2015).
[78] S. Niu, S. Wang, L. Lin, Y. Liu, Y. S. Zhou, Y. Hu, and Z. L. Wang, Energy Environ. Sci. **6**(12), 3576 (2013).
[79] Y. S. Zhou, G. Zhu, S. Niu, Y. Liu, P. Bai, Q. Jing, and Z. L. Wang, Adv. Mater. **26**(11), 1719 (2014).
[80] Y. S. Zhou, Y. Liu, G. Zhu, Z.-H. Lin, C. Pan, Q. Jing, and Z. L. Wang, Nano Lett. **13**(6), 2771 (2013).
[81] Y. S. Zhou, S. Wang, Y. Yang, G. Zhu, S. Niu, Z.-H. Lin, Y. Liu, and Z. L. Wang, Nano Lett. **14**(3), 1567 (2014).
[82] G. Zhu, Z.-H. Lin, Q. Jing, P. Bai, C. Pan, Y. Yang, Y. Zhou, and Z. L. Wang, Nano Lett. **13**(2), 847 (2013).
[83] C. K. Jeong, K. M. Baek, S. Niu, T. W. Nam, Y. H. Hur, D. Y. Park, G.-T. Hwang, M. Byun, Z. L. Wang, Y. S. Jung, and K. J. Lee, Nano Lett. **14**(12), 7031 (2014).
[84] H. G. Yoo, M. Byun, C. K. Jeong, and K. J. Lee, Adv. Mater. **27**(27), 3982 (2015).
[85] C. K. Jeong, H. M. Jin, J.-H. Ahn, T. J. Park, H. G. Yoo, M. Koo, Y.-K. Choi, S. O. Kim, and K. J. Lee, Small **10**(2), 337 (2014).
[86] S. Wang, Y. Xie, S. Niu, L. Lin, C. Liu, Y. S. Zhou, and Z. L. Wang, Adv. Mater. **26**(39), 6720 (2014).
[87] Y. Yu, Z. Li, Y. Wang, S. Gong, and X. Wang, Adv. Mater. **27**(33), 4938 (2015).
[88] S. Wang, Y. Zi, Y. S. Zhou, S. Li, F. Fan, L. Lin, and Z. L. Wang, J. Mater. Chem. A **4**(10), 3728 (2016).
[89] G. Zhu, B. Peng, J. Chen, Q. Jing, and Z. L. Wang, Nano Energy **14**, 126 (2015).
[90] A. Li, Y. Zi, H. Guo, Z. L. Wang, and F. M. Fernandez, Nat. Nanotechnol. (in press).
[91] S. Wang, Z.-H. Lin, S. Niu, L. Lin, Y. Xie, K. C. Pradel, and Z. L. Wang, ACS Nano **7**(12), 11263 (2013).
[92] J. Luo, F. R. Fan, T. Jiang, Z. Wang, W. Tang, C. Zhang, M. Liu, G. Cao, and Z. L. Wang, Nano Res. **8**(12), 3934 (2015).
[93] J. Wang, X. Li, Y. Zi, S. Wang, Z. Li, L. Zheng, F. Yi, S. Li, and Z. L. Wang, Adv. Mater. **27**(33), 4830 (2015).
[94] Y. Zi, J. Wang, S. Wang, S. Li, Z. Wen, H. Guo, and Z. L. Wang, Nat. Commun. **7**, 10987 (2016).
[95] L.-C. Luo, D.-C. Bao, W.-Q. Yu, Z.-H. Zhang, and T.-L. Ren, Sci. Rep. **6**, 19246 (2016).
[96] S. Niu, X. Wang, F. Yi, Y. S. Zhou, and Z. L. Wang, Nat. Commun. **6**, 8975 (2015).
[97] Y. Zi, H. Guo, J. Wang, Z. Wen, S. Li, C. Hu, and Z. L. Wang, Nano Energy **31**, 302 (2017).
[98] N. Adroja, S. B. Mehta, and P. Shah, J. Emerging Technol. Innovative Res. **2**(3), 847–850 (2015), see http://www.jetir.org/view?paper=JETIR1503089.
[99] R. G. Kepler and R. A. Anderson, J. Appl. Phys. **49**(8), 4490 (1978).
[100] T. Furukawa, J. X. Wen, K. Suzuki, Y. Takashina, and M. Date, J. Appl. Phys. **56**(3), 829 (1984).
[101] X. Li, S.-G. Lu, X.-Z. Chen, H. Gu, X.-shi. Qian, and Q. M. Zhang, J. Mater. Chem. C **1**(1), 23 (2013).
[102] Y. Yang, J. H. Jung, B. K. Yun, F. Zhang, K. C. Pradel, W. Guo, and Z. L. Wang, Adv. Mater. **24**(39), 5357 (2012).
[103] Q. Leng, L. Chen, H. Guo, J. Liu, G. Liu, C. Hu, and Y. Xi, J. Mater. Chem. A **2**(30), 11940 (2014).
[104] S. B. Lang, Phys. Today **58**(8), 31 (2005).
[105] Y. Yang, S. Wang, Y. Zhang, and Z. L. Wang, Nano Lett. **12**(12), 6408 (2012).
[106] Y. Yang, Z.-H. Lin, T. Hou, F. Zhang, and Z. L. Wang, Nano Res. **5**(12), 888 (2012).
[107] F. H. J. van der Heyden, D. Stein, and C. Dekker, Phys. Rev. Lett. **95**(11), 116104 (2005).
[108] M. Z. Bazant and T. M. Squires, Phys. Rev. Lett. **92**(6), 066101 (2004).
[109] Z. L. Wang, "*On Maxwell's displacement current for energy and sensors: the origin of nanogenerators,*" Mater. Today (to be published).